Physikalisches Praktikum für Fortgeschrittene (P3)

Elektrische Leitfähigkeit von Festkörpern bei tiefen Temperaturen

Betreuer: Dr. Lukashenko

Michael Lohse, Matthias Ernst
Gruppe 11

Karlsruhe, 8.11.2010

The aim of this experiment is the measurement and understanding of the temperature dependence of the resistances of metals, superconductive metals and semiconductors. Samples of copper, niobium and phosphorous-doped silicon are studied. To achieve the low temperatures needed for superconductivity of niobium, helium-cooling is applied.

1 Theoretical Foundations

1.1 Electrical resistance of metals

The electrical resistance can easily be understood in a classical way in the context of a theory by Drude. Electrons that are accelerated by an electrical field E are scattered at the atom cores in the lattice after a relaxation time τ and loose their entire energy gained from the field. On average, the electrons (with charge e and mass m_e move with a constant drift velocity

$$v_\mathrm{D} = \frac{-eE}{m_\mathrm{e}}\tau \tag{1}$$

Using the current density $j = -env_\mathrm{D}$ with the electron density n, the conductivity is

$$\sigma = \frac{ne^2\tau}{m_\mathrm{e}} \tag{2}$$

For the relaxation rate τ^-1, scattering rates at the lattice (phonons, τ_Ph^{-1}) and at lattice defects (τ_{St}^{-1}) have to be considered: $\tau^{-1} = \tau_\mathrm{Ph}^{-1} + \tau_{St}^{-1}$. This can used to express the specific resistance $\rho = \sigma^{-1}$ with the Mathiesen rule as

$$\rho = \rho_\mathrm{Ph}(T) + \rho_\mathrm{St} \tag{3}$$

For very low temperatures $T \to 0$, there is no phonon scattering, only a residual resistance caused by lattice defects remains independent on temperature. For temperatures below the Debye temperature $T \ll \Theta$ where all phonons are excited, the dependence of resistance is $\rho_\mathrm{Ph}(T) \propto T^5$. The rapid decrease is due to the loss of phonon excitation. For high temperatures $T \gg \Theta$, resistance increases linearly with temperature: $\rho_\mathrm{Ph}(T) \propto T$.

For high temperatures $T \gg \Theta$, the following dependence found by Grüneisen and Borelius holds:

$$R_\mathrm{T}(T) = 1.17\frac{R_\Theta}{\Theta}T - 0.17R_\Theta \tag{4}$$

where R_Θ is the resistance at the Debye temperature. Furthermore, the Mathiesen rule has to be taken into account, $R = R_\mathrm{res} + R_\mathrm{T}(T)$.

1.2 Conductivity of semiconductors

Semiconducturs show a gap between valence band and conductance band that is rather small. At low temperatures, the conductance band is almost empty and therefore the resistance of the semiconductor is high. When temperature increases, electrons are excited from valence band into conductance band because of thermal energy, the semiconductor thus becomes conductive.

For *intrinsic* semiconductors, the band gap of energy E_g has to be overcome and no further effects play a role. Conductance results both from excited electrons and left-over holes in the

valence band. In total, conductivity and resistance of intrinsic semiconductors at temperature T can be expressed as

$$\begin{aligned} \sigma_\mathrm{i} &= C_\mathrm{i} \mathrm{e}^{-\frac{E_\mathrm{g}}{2kT}} \\ R &= R_\mathrm{min} e^{\frac{E_\mathrm{g}}{2kT}} \end{aligned} \tag{5}$$

with the Boltzmann constant k and material-dependent constants C_i and R_min.

In constrast, *extrinsic* semiconductors show a more complicated behaviour because here, the seminconductor is doped with other atoms with more or less electrons, acting as electron donators (n-doped semiconductors) or acceptors (p-doped semiconductors). This is particular important at low temperatures, where conductance is significantly larger than with intrinsic semiconductors. At high temperatures, effects of thermal excitation become more important and thus, extrinsic and intrinsic semiconductors show the same behaviour in high-temperature limes. The full temperature dependence of extrinsic semiconductors is rather complicated, as it consists of several parts that play a main role in a certain temperature range each. A sample can be found in the preparation folder (fig. 2, page 14f).

1.3 Superconductivity

Some materials show a sharp drop in their electrical resistance to zero below a certain critical temperature T_c. This phenomenon is called superconductivity and was discovered experimentally more than 100 years ago. Because of this sharp transition, it can be considered as phase transition, expressed by an order parameter of the eletrons. Critical temperatures for metallic superconductors are around $0 - 10\mathrm{K}$. Other superconductors with more complicated structures like YBaCo show critical temperatures up to 150K.

1.4 BCS-theory

An explanation for superconductivity has been given by Bardeen, Cooper and Schrieffer (BCS-theory). Electrons moving through an atomar lattice can polarize this lattice. The polarization can now act on another electron, thus creating a correlation between these two electrons that is attrative and larger than their Coulombic repulsion. This correlation is transmitted by phonons and is called Cooper pair. A Cooper pair consists of two electrons of opposite spin, $(\vec{p}\uparrow, -\vec{p}\downarrow)$. In total, it has a spin of 0 and is therefore a boson. Unlike fermions (as electrons), several bosons can be in the same state, mainly the ground state. In the BCS theory, a close correlation between all cooper pairs is postulated, they have to be in the same quantum mechanical state. Because of this, interaction like momentum transfer can not act on a single Cooper pair but has to act on all Cooper pairs at once. Because this is impossible, electrons can not exchange momentum with the lattice, so there is no resistance of the electric current in a superconductor.

To break a Cooper pair, the according energy of the correlation is needed. This energy can either be thermal energy that increases the momentum of all cooper pairs so they finally collapse or can be supplied by a magnetic field. If a magnetic field is applied to a superconductor, a current is induced. Unlike in usual conductors, where this current weakens very fast because of the resistance of the conductor, the induced current in a superconductors stays permanent as the resistance vanishes. Furthermore, the induced current creates an internal magnetic field that has the same absolute value as the external so it cancels this inside of the superconductor except for a thin layer of thickness λ on the surface. This phenomenon is called Meissner effect (in german Meißner-Ochsenfeld Effekt). When the external magnetic field reaches a certain value, the Meissner

effect breakes down (of course, the critical magnetic field also depends on temperature). Because of the Meissner effect, a superconductor can be considered as perfect diamagnet, so the magnetic susceptibility vanishes,

$$\chi = \frac{\mu_0 M}{B} = -1 \tag{6}$$

with the magnetization M, the magnetic field B and the vacuum permeability μ_0. Superconductors with a critical magnetic field at which superconductivity collapses at once and the Meissner effect no longer holds are called type I superconductors. Some superconductors, termed type II superconductors show a different behaviour. At low temperatures, the Meissner effect can be observed. At a lower critical field B_{c1}, they enter a state called Shubnikov phase where the magnetic field is not repelled completely from the inside of the superconductor but enter it in so called vortices. This gradually weakens superconductivity until a second critical magnetic field B_{c1} where it collapses.

1.5 GLAG-theory

A phenomenological treatment of superconductivity has been given by Ginsburg, Landau, Abrikosov and Gorkov (GLAG-theory). Two characteristic lengths are crucial: the penetration depth λ, where the magnetic field has dropped to the fraction of $\frac{1}{e}$ of its outer value found to be

$$\lambda(T) = \lambda(0)\left(1 - \left(\frac{T}{T_{\mathrm{c}}}\right)^4\right)^{-\frac{1}{2}} \tag{7}$$

and the Ginsburg Landau coherence length, describing thermodynamic fluctuations of the cooper pairs is determined as

$$\xi_{\mathrm{GL}}(T) = \frac{\xi_{\mathrm{GL}}^{(0)}}{\sqrt{1 - \frac{T}{T_{\mathrm{c}}}}} \tag{8}$$

The coherence length at $T = 0\mathrm{K}$ is given by

$$\xi_{\mathrm{GL}}^{(0)} = \left(\frac{-\Phi_0}{2\pi S T_{\mathrm{c}}}\right)^{\frac{1}{2}} \tag{9}$$

with the flux quantum $\Phi_0 = 2-07 \cdot 10^{-15}\mathrm{V\,s}$ and the slope $S = \left.\frac{\mathrm{d}B_{\mathrm{c2}}}{\mathrm{d}T}\right|_{T=T_{\mathrm{c}}}$ of the critical magnetic field B_{c2}

$$\begin{aligned} B_{\mathrm{c2}}(T) &= \frac{\Phi_0}{2\pi\xi_{\mathrm{GL}}^2(T)} = \frac{\Phi_0}{2\pi {\xi_{\mathrm{GL}}^{(0)}}^2}\left(1 - \frac{T}{T_{\mathrm{c}}}\right) \\ \Rightarrow S &= \left.\frac{\mathrm{d}B_{\mathrm{c2}}}{\mathrm{d}T}\right|_{T=T_{\mathrm{c}}} = \frac{-\Phi_0}{2\pi {\xi_{\mathrm{GL}}^{(0)}}^2 T_{\mathrm{c}}} \end{aligned} \tag{10}$$

With the Ginsburg Landau parameter $\kappa = \frac{\lambda}{\xi_{\mathrm{GL}}}$, superconductors can be classified. For type I superconductors, κ is found to be $\kappa < \frac{1}{\sqrt{2}}$, for type II superconductors $\kappa > \frac{1}{\sqrt{2}}$. Niobium which we will use as sample is just at the border of those two types, depending on the number of lattice defects.

2 Experimental Setup

All measurements are carried out in a cryostat, shown in figure 4 of the preparation folder. This cryostat consists of two double-walled glass dewars. The outer dewar is filled with liquid nitrogen, thus able to cool the samples down to at most 77K. The inner dewar is then filled with liquid helium, so the samples can be cooled to at most 4K and superconductivity of the niobium sample can be reached. Inside of the inner dewar, a sample holder and a heater are attached. The sample holder is sourrounded by a superconductive coil, for a normal conducting coil would vapour the liquid helium because of the Joule heat in a short time.

Temperature can be taken via a platinum sensor that is able to properly measure temperature down to about 50K because of the mainly linear dependece of resistance on current and a carbon sensor, for which resistance increases at lower temperatures thus enabling us to gauge low temperatures accurately.

Three samples are to be measured: a copper sample as metal, a phosphorus-doped silicon sample as a semi-conductor and a niobium sample. We expect these interdependece of the resistance on temperature:

- Copper sample: Copper is a typical metal, so we expect a linearity at high temperatures. At about the Debye temperature, we expect a proportionality of $R \propto T^5$. At lower temperatures, this should turn into a constant, the residual resistance.
- Silicon sample: Phosphorus-doped silicon is a semiconductor. We therefore expect an inverse exponential correlation of resistance and temperature, so the resistance at low temperatures ought to be very high.
- Niobium sample: Niobium is a metal which becomes superconductive at $T_\mathrm{C} = 9.2K$. We can observe this transition because of the helium cooling, so we expect a similar shape as for copper, except for a drop from the residual resistance to $R = 0\Omega$ at about that temperature.

3 Procedure

After we had been introduced to the experimental setup by the supervisor, we evacuated the inner dewar and its walls to avoid water residues, then refilled the walls with a small amount of helium and flushed the inner dewar with helium. We then filled the outer dewar with liquid nitrogen to cool down the samples.

We began taking data at about 4,5°C. Unfortunately, we forgot to measure the resistances of the samples and thermometers at room temperature. The highest values we measured seemed to be in reasonable agreement to the values in the preparation folder. Furthermore, we have been able to extrapolate most of these values because of the expected and observed linear dependence of resistance on temperature. Doing this, we obtain $R_\mathrm{Cu} = 2.43\Omega$, $R_\mathrm{Nb} = 50.82\Omega$, $R_\mathrm{Si} = 0.09\Omega$ and $R_\mathrm{Pt} = 109.54\Omega$. These are a little bit different from the values provided in the preparation folder, but not very much.

At about 200K, we poured liquid helium to the inner dewar to speed up the cooling process. Because the temperature dropped so fast, we could not write down the values as before but we were able to take pictures of the displays from which we gained proper values of this fast cool-down. At about 55K, we switched from platinum to carbon sensor for proper temperature measurement.

To determine the dependence of the critical temperature on the magnetic field, we used a plotting device to gain the resistance-temperature-curve for different magnetic fields. We increased the

current through the superconductive coil from 0A to 12A in steps of 1.5A. Each time, we heated the sample so it lost superconductivity and plotted the cool-down curve. We noticed a linear decrease of resistance on increasing magnetic field as expected.

Finally, we used the heater to slowly increase temperature of the samples to about 150K an took resistance values again to gain more accurate data in that domain.

4 Analysis

The values we measured for the resistance curves are the voltages that dropped on each sample by providing each one with a current of $I = 1\text{mA}$. The resistance is then easily computed via $R = \frac{U}{I}$.

4.0.1 Some words on error calculation

In principle, we would have to to error propagation and thereby calculate systematical and statistical errors of all values we measured. Unfortunately, the manual did not define any errors of the measuring units. In particular, we don't know anything about the errors in the thermal sensors we are using and the fitted functions supplied in the manual that we have to use to compute the temperature are also mainly given without any error estimates. So we could only guess systematical errors in our experiment but as we do not know the experimental setup and its capabilities very well, we do not want to speculate on numbers and so a specification of systematical errors is impossible. It seems though that systematical errors are quite small or being compensated as most of our results appear quite reasonable.

In course of the many linear regressions we performed, statistical errors have been obtained as well. We will declare those with the values of the fits but we will not perform any error propagation as this is only part of the entire error and we can not do error calculation on systematical errors as just explained.

4.1 Resistance graphs

Figure 1 shows the resistance graph for the three samples we measured. As one can clearly see, Niobium has a rather high resistance that decreases with decreasing temperature and drops to zero at about 5K. Copper has a quite low resistance that steadily decreases and the Si:P sample shows a very low resistance at high temperatures but with a sharp increase at about 4K.
To investigate the shapes of the resistance curves in more detail, these are shown in a single graph each.

Figure 2 shows our results for the copper sample. The linear dependence of the resistance on the temperature from room temperature to about 55K can clearly be seen. The slightly bent shape (red) of the cool down curve between 55K and 200K is due to the addition of liquid helium. This considerably speeded up the cool-down process so our measurements obviously did not take place in thermal equilibrium. Later, when whe heated the samples more slowly and took the values again, the linear developing of the values is much better (yellow curve). At lower temperatures than about 50K, the linearity changes to a more curved shape and becomes constant at about 30K. To analyze the domain of low temperatures, the range between 0K and 70K is depicted in figure 3.

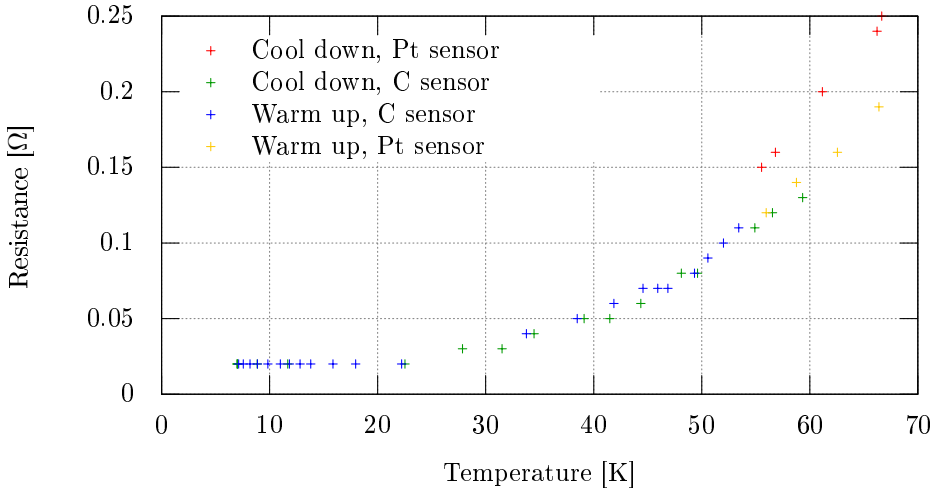

Figure 3: Resistance graph of Copper sample at lower temperatures

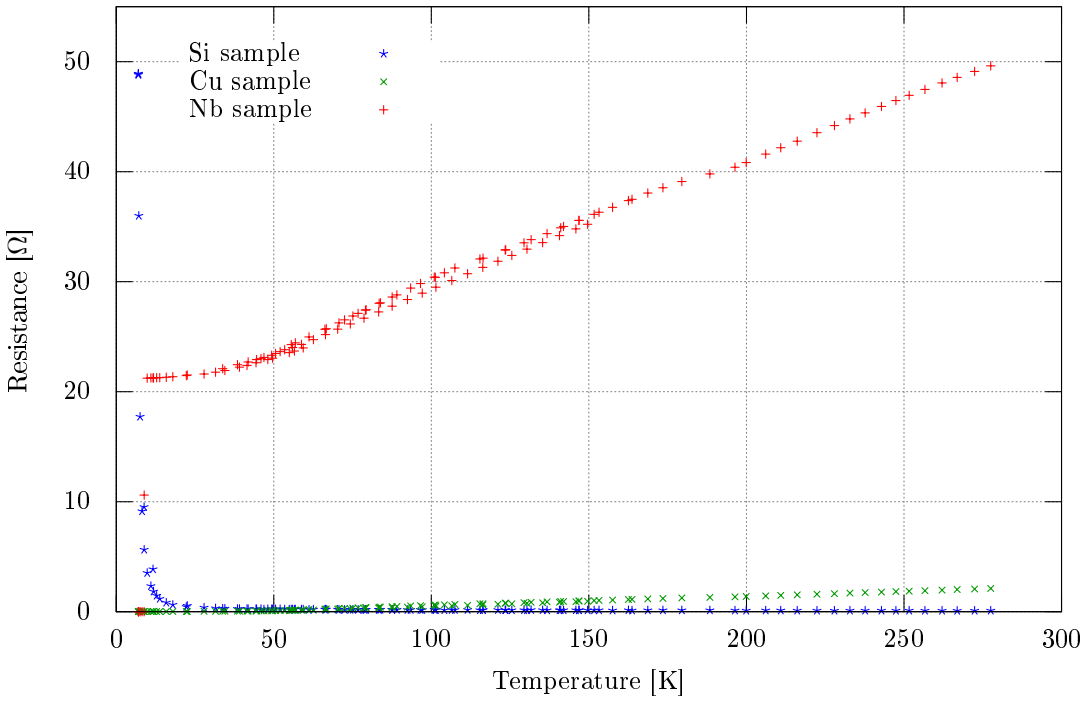

Figure 1: Resistance graph of all measured samples

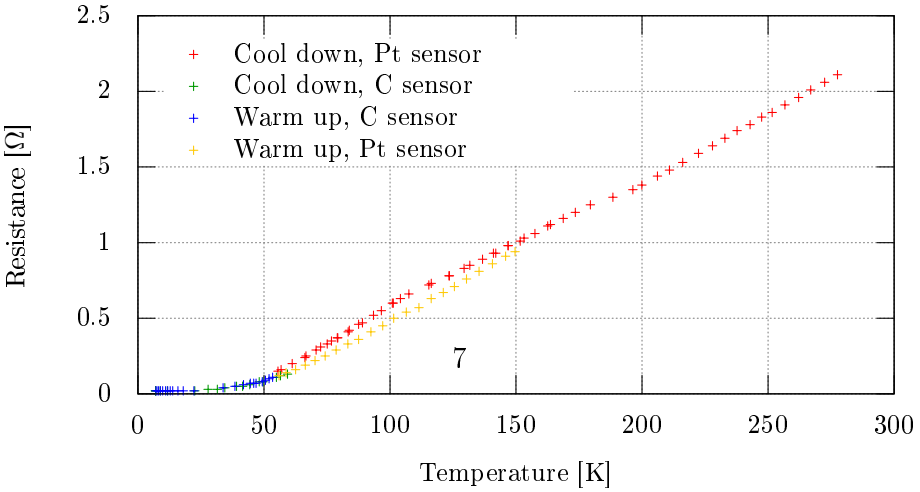

Figure 2: Resistance graph of Copper sample

There, the non-linear behavior within a certain range (this will be discussed later) and the low but nevertheless non-vanishing residual resistance can be seen.

The graph of the niobium sample is shown in figure 4.

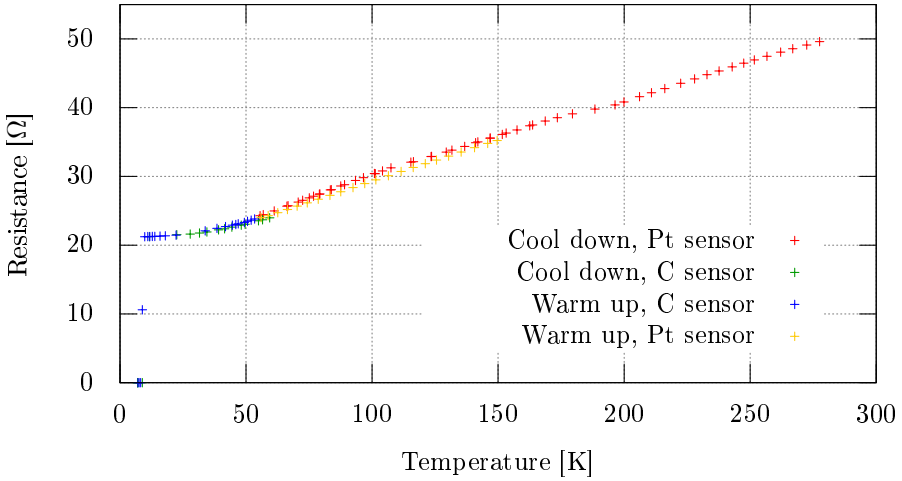

Figure 4: Resistance graph of Niobium sample

Despite the overall higher resistance of niobium, the associated curve resembles the one of the copper sample except at very low temperatures. There, the transition to the superconductive state with a vanishing resistance is obious. For niobium, too, the low temperature domin are upscaled and shown in figure 5.

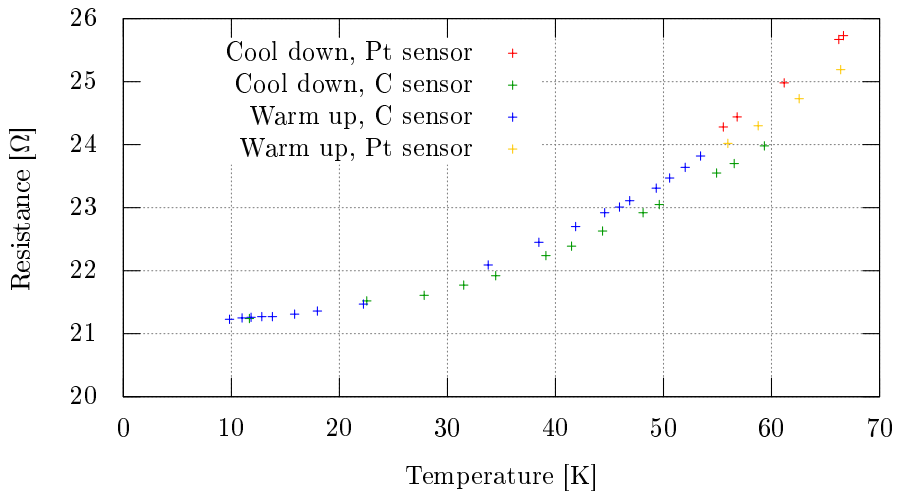

Figure 5: Resistance graph of Niobium sample at lower temperatures

Note that the transition to the superconductive state is not shown. Here, too, we see the residual resistance before this transition and the non-linear behavior.

Finally, the graph of the silicon sample is shown in figure 6. The scaling is logarithmic on both axes.

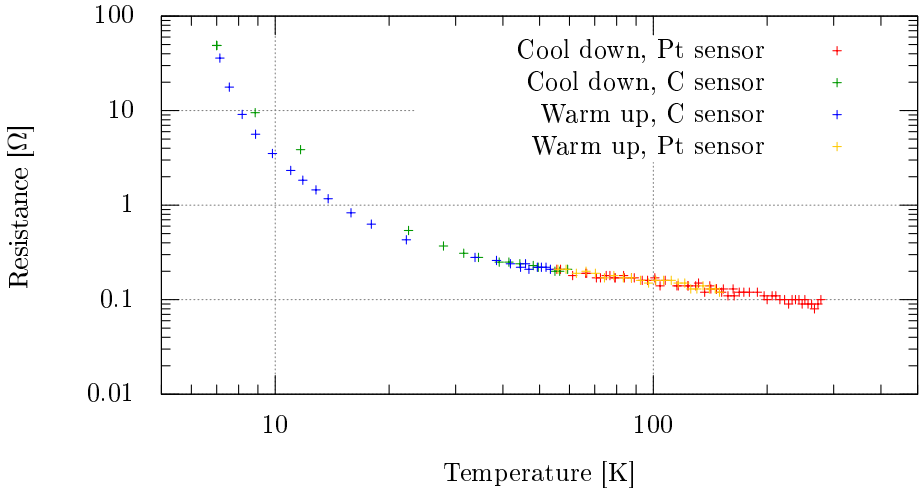

Figure 6: Resistance graph of Phosphorous doped Silicon sample

For silicon, a very different shape than ones of the metallic samples has to be stated. As already pointed out and in agreement to our expectation, the resistance of silicon increases almost imperceptibly with decreasing temperature and then sharply increases. This behaviour results in the semiconducting nature of silicon.

4.2 Debye temperatures and power of non-linear temperature-resistance dependence

To obtain the Debye temperature Θ and the Debye resistance $R(\Theta)$, we use the Grüneisen-Borrelius-equation:

$$R_T(T) = 1.17\frac{R_\Theta}{\Theta}T - 0.17R_\Theta \tag{11}$$

As the Matthiesen rule holds, $R = R_{\text{res}} + R_T(T)$, we have to subtract the residual resistance from the measured values to get the correct results.

$$R_T(T) = \underbrace{1.17\frac{R_\Theta}{\Theta}}_{m}\,T\,\underbrace{-0.17R_\Theta + R_{\text{res}}}_{c} \tag{12}$$

Then, we can perform a linear regression and use the values the axis intercept c and for the slope m to gain the values of interest by $R_\Theta = (R_{\text{res}} - c)/0.17$ and $\Theta = 1.17R_\Theta/m$.

The residual resistances were taken from the lowest values we measured. For the copper sample, these remained constant at $R_{\text{res,Cu}} = 0.02\Omega$ from 22K to 7K. For niobium, we used the last value measured before the transition to superconductivity, so $R_{\text{res,Nb}} = 21.23\Omega$.

The linear regression graph for copper is displayed in picture 7.

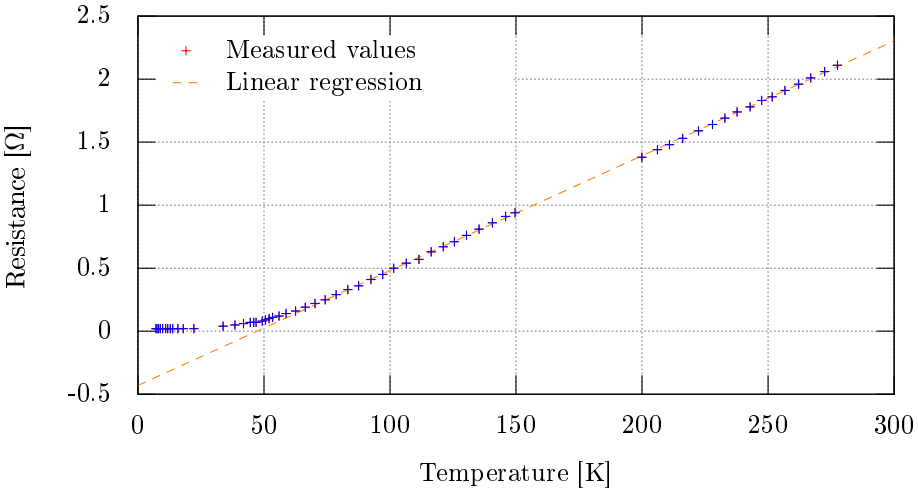

Figure 7: Linear regression of copper at higher temperatures

We used the values during cooling down before we added helium and the values during warming-up from 70K upwards, where our data suited the suggested linearity very well. This corresponds to the values for $m = (0.009114 \pm 0.000017)\Omega/\mathrm{K}$ and $c = (-0.4304 \pm 0.0033\Omega)$. We therefore obtain

$$\begin{aligned} \Theta &= 340.12\mathrm{K} \\ R_\Theta &= 2.65\Omega \end{aligned} \tag{13}$$

The very small statistical errors of these values can be neglected as the instrumental error is assumed to be much larger. Nevertheless, our results is in surprising agreement to published data of $\Theta = 343.5K$ (C. Kittel, Introduction to Solid State Physics, 7th Ed., Wiley, 1996).

With the same procedure, we can calculate Θ and R_Θ for niobium. The linear regression graph is supplied in fig. 8.

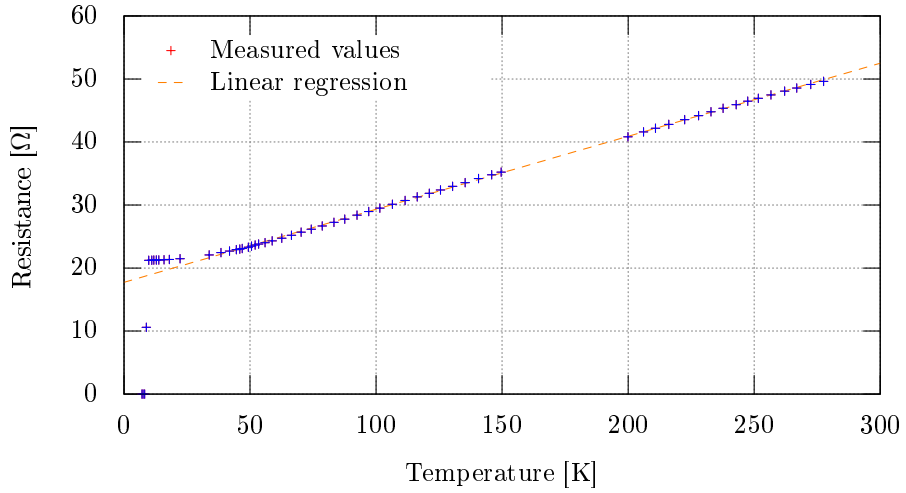

Figure 8: Linear regression of niobium at higher temperatures

Linear regression yields $m = (0.11589 \pm 0.00028)\Omega/\mathrm{K}$ and $c = (17.733 \pm 0.052\Omega)$. This corresponds to

$$\begin{aligned} \Theta &= 207.67\mathrm{K} \\ R_\Theta &= 20.57\Omega \end{aligned} \tag{14}$$

These values are in rather bad agreement to published data[1] of $\Theta = 275\mathrm{K}$, mainly due to the uncertainty in the residual resistance that could not be as properly determined as for copper. If we assume $R_{\mathrm{res,Nb}} = 22.3\Omega$, just 5% larger, the resulting Debye temperature is 271.22K which is a much better result.

To verify Grüneisen-Borrelius-equation (eq. 11), we show the data of the copper and niobium samples in reduced units in figure 9, i.e. we plotted $(R - R_{\mathrm{res}})/R_\Theta$ over T/Θ for both species.

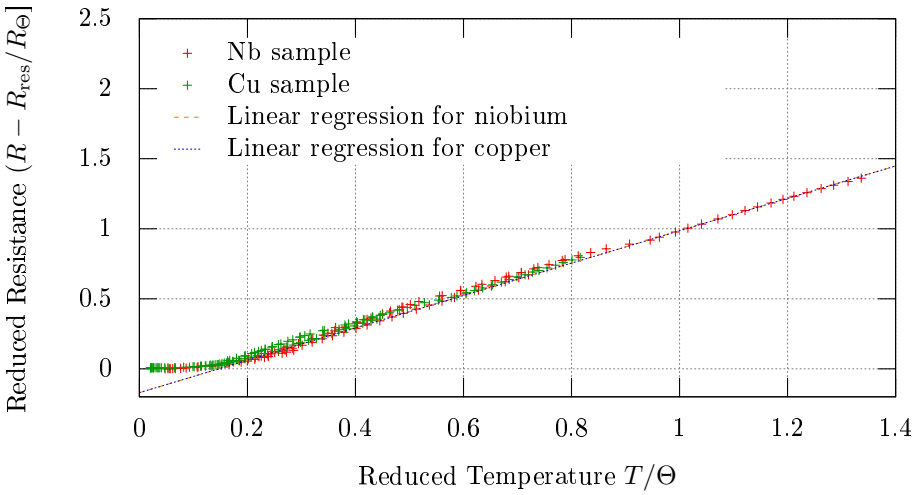

Figure 9: Linear regression of niobium at higher temperatures

The linear depedence at higher temperatures can clearly be seen, whereas at low temperature, the residual resistance is achieved. Linear regression from $T/\Theta = 0.3$ on yields

$$R_T(T) = (1.1717 \pm 0.0033)\frac{R_\Theta}{\Theta}T - (0.1637 \pm 0.0020)R_\Theta \qquad \text{for the copper sample and}$$

$$R_T(T) = (1.1564 \pm 0.0029)\frac{R_\Theta}{\Theta}T - (0.1704 \pm 0.0025)R_\Theta \qquad \text{for the niobium sample.}$$

Here, we used all the data for linear regression, not only the data obtained during high-temperature cool-down and warming-up phase, so our result is in good agreement with the expectation.

To finally check the power p in the nonlinear region as $R \propto T^p$, we did a double-logarithmic plot of both copper (fig. 10) and niobium (fig. 11) and a linear regression in each diagram. We used only the lowest values for the regression.

[1] Source: http://chemistry.about.com/od/elementfacts/a/niobium.htm

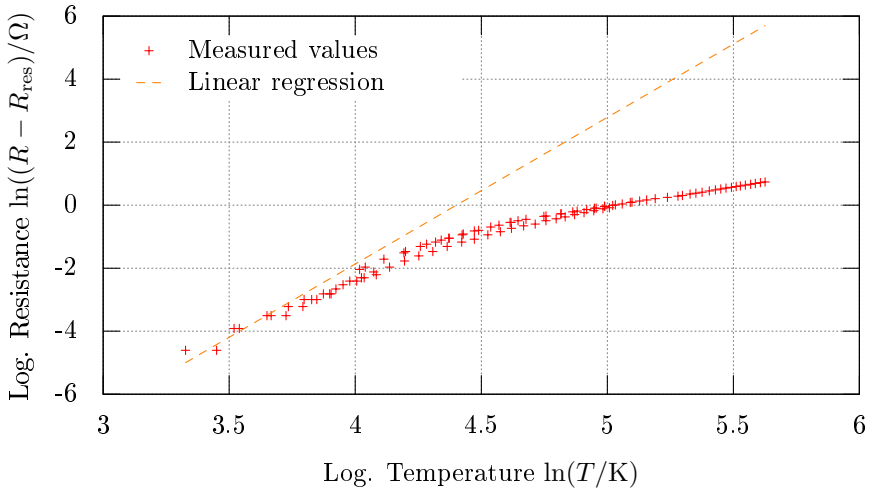

Figure 10: Double-logarithmic graph for copper

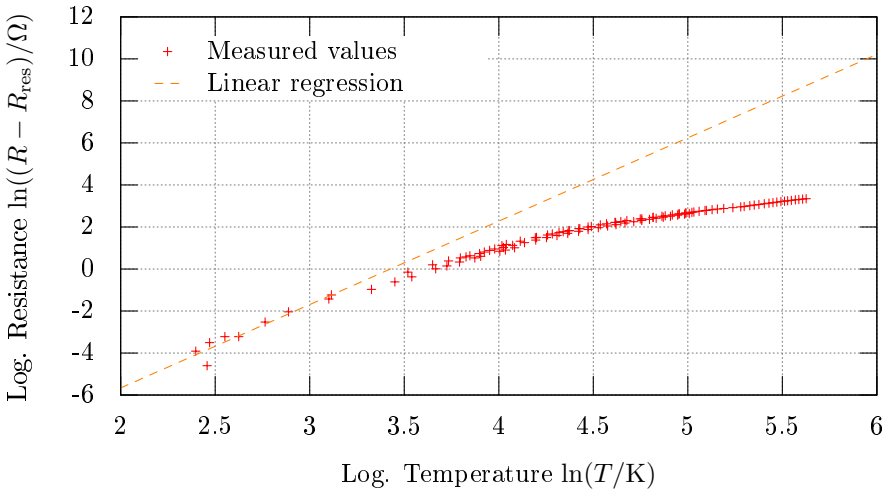

Figure 11: Double-logarithmic graph for niobium

We get $p_{\mathrm{Cu}} = 4.65 \pm 0.93$ and $p_{\mathrm{Cu}} = 3.97 \pm 0.43$. In both cases, we do not have enough data in the non-linear region and those we have are widely scattered, so the fit is based on very few points. This explains the difference from the expected power $p_{\mathrm{ex}} = 5$.

4.3 Specific resistances and mean free paths

To calculate the specific resistances of our copper and niobium samples, we use the definition of the specific resistance ρ:

$$\rho(T) = R(T)\frac{A}{l} \tag{15}$$

with the electrical resistance R, the cross section A and the lenght l of the sample under consideration. If we assume the dimensions of the samples to be independent on temperature, we can

calculate those with the values given in the preparation folder and then calculate the specific resistance at low temperatures using the residual resistances determined above. Knowing the specific resistance, the mean free path ℓ can be calculated via $\ell = \frac{\rho\ell}{\rho}$ with the values of $\rho\ell$ given in the manual.

For the copper sample, the following values are given in the preparation folder:

$$\rho_{\mathrm{Cu}}(300\mathrm{K}) = 1.71 \cdot 10^{-8}\Omega\,\mathrm{cm} \qquad \rho\ell = 658.7 \cdot 10^{-18}\Omega\mathrm{m}^2$$
$$d = 1 \cdot 10^{-4}\mathrm{m} \Rightarrow A_{\mathrm{Cu}} = \pi\left(\frac{d}{2}\right)^2 = 7.85 \cdot 10^{-9}\mathrm{m}^2$$

To calculate the resistance of copper at 300K, we use the Grüneisen-Borrelius-equation 12 with the values we found above, $\Theta_{\mathrm{Cu}} = 340.12\mathrm{K}$, $R_{\Theta,\mathrm{Cu}} = 2.65\Omega$ (see eq. 13) and $R_{\mathrm{res,Cu}} = 0.02\Omega$. We obtain $R(300\mathrm{K}) = 2.30\Omega$ and, with equation 15, $l_{\mathrm{Cu}} = \frac{RA}{\rho} = 1.06\mathrm{m}$. Using the residual resistance and the assumption of temperature-independent sample volume, we get $\rho_{\mathrm{Cu}}(4.2\mathrm{K}) = 1.48 \cdot 10^{-10}\Omega\,\mathrm{m}$. The mean free path at $T = 4.2\mathrm{K}$ is then

$$\ell_{\mathrm{Cu,4.2K}} = \frac{\rho\ell}{\rho} = \frac{658.7 \cdot 10^{-18}\Omega\mathrm{m}^2}{1.48 \cdot 10^{-10}\Omega\,\mathrm{m}} = 4.44 \cdot 10^{-6}\Omega = 4.44\mu\Omega \tag{16}$$

This rather high value compared to atomar dimension shows us that at this low temperature, the atoms are mainly "frozen" so collisions of electrons with atoms are much less probable than at room temperature so the mean free path is rather long.

For niobium, we can find the following values in the preparation folder:

$$\rho\ell = 375 \cdot 10^{-18}\Omega\mathrm{m}^2 \qquad l = 8 \cdot 10^{-3}\mathrm{m}$$
$$w = 9 \cdot 10^{-4}\mathrm{m} \quad s = 40 \cdot 10^{-9}\mathrm{m} \quad \Rightarrow A_{\mathrm{Nb}} = w \cdot s = 3.60 \cdot 10^{-11}\mathrm{m}^2$$

As the length is given, we only need to calculate the specific resistance $\rho_{\mathrm{Nb}}(12\mathrm{K}) = 9.55 \cdot 10^{-8}\Omega\mathrm{m}$. Using this, we get

$$\ell_{\mathrm{Nb,12K}} = 3.93 \cdot 10^{-9}\mathrm{m} = 3.93\mathrm{nm} \tag{17}$$

This value is much smaller than the one found for copper (corresponding to the much higher residual resistance). We see that the transition to superconductivity that occurs only 3Kbelow and where the mean free path is infinity requires an abrupt phase transition.

4.4 Superconductivity of Niobium

Now, we want to determine the temperature dependency of the upper critical magnetic field B_{c2}. As described above, we used the supplied device which plotted the voltage that dropped on the niobium sample. After we had calibrated the device, we disabled the plotter, heated the sample so it lost superconductivity, reenabled the plotter and let the sample cool down below the critical temperature. We did that several times, where we increased the current through the superconducting coil from 0A to 12A in steps of 1.5A.
In the plots, we could not see a very sharp transition but rather a smoothed shape. We therefore used the points where the voltage had dropped to the half of its initial value to calculate the critical temperatures. The magnetic field is computed by the formula given in the manual,

$$B = \mu_0 \frac{n}{2l} I \left(\frac{x + l/2}{\sqrt{r^2 + (x + l/2)^2}} - \frac{x - l/2}{\sqrt{r^2 + (x - l/2)^2}} \right) \tag{18}$$

with the number of folds $n = 4019$, the length $l = 10\text{cm}$ and the mean radius $r = 1.925\text{cm}$ of the coil. As we do not know exactly where our sample is located inside the coil, we assume it to be in the middle, so $x = 0$ and the field is homogeneous at the position of the sample. As calibration, we used the lowest temperature we could achieve as origin and measured the differences to higher temperatures. The values obtained are summarized in table 1 and depicted in figure 12. There,

I [A]	0	1.5	3.0	4.5	6.0	7.5	9.0	10.5	12
B_{c2} [mT]	0.0	70.7	141.4	212.1	282.8	353.5	424.2	494.9	565.6
R [Ω]	988	1012	1029	1051	1072	1091	1111	1129	1145
T [K]	9.02	8.83	8.7	8.54	8.4	8.28	8.15	8.05	7.95

Table 1: Critical magnetic field for niobium sample

we can observe almost linearity between the critical magnetic field B_{c2} and temperature T. With increasing temperature, the magnetic field decreases. This is what we expect since the energy needed to break the Cooper pairs ans so destroy supercondictivity can origin from thermal or magnetical energy. If the magnetic field is stronger, less thermal energy is needed and therefore, T_c is lower.

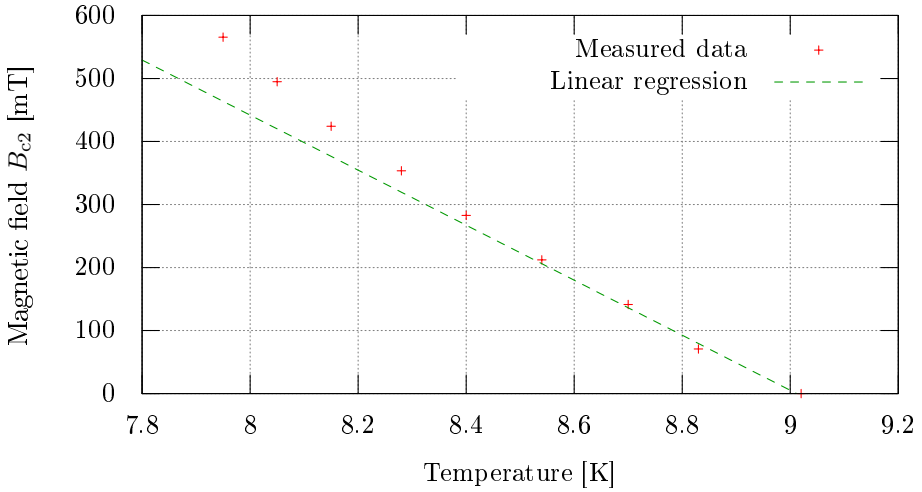

Figure 12: Measurement of critical magnetic field and temperature

Intending to calculate the coherence length, we did a further linear regression. This time, we used only the last three points as indicated in the manual, for the following formula deduced in the Ginsburg Landau theory holds only near the transition temperature T_C:

$$\xi_{GL}^{(0)} = \sqrt{\frac{-\Phi_0}{2\pi S T_c}} \tag{19}$$

with the flux quantum $\Phi_0 = 2.07 \cdot 10^{-15}\text{V s}$ and the slope $S = (-436 \pm 47)^{\text{mT}}/\text{K}$ of the linear regression line. We used the temperature without magnetic field $T_c = 9.02\text{K}$ as T_c and get $\xi_{GL}^{(0)} = 9.15 \cdot 10^{-9}\text{m} = 9.15\text{nm}$. Hereby, we can calculate the mean free path one more time by $\ell = \frac{(\xi_{GL}^{(0)})2}{39\text{nm}} = 2.15\text{nm}$. This is only about half of the value determined before.

4.5 Activation energy of Silicon

Finally, we want to determine the activation energy of Silicon. As we use the 4-point probes method with length l and cross section A, we can calculate the conductivity as $\sigma = \frac{L}{R \cdot A}$. Furthermore, the conductivity of intrinsic semiconductors is $\sigma = C \cdot exp\left(\frac{E_a}{2k_B T}\right)$, so we have

$$\begin{aligned} \frac{l}{R \cdot A} &= C \mathrm{e}^{-\frac{E_a}{2k_B T}} \\ \Rightarrow \ln R &= E_A \frac{1}{2k_B T} + \ln \frac{A \cdot C}{l} \end{aligned} \tag{20}$$

If we now plot $\ln R$ over $\frac{1}{2k_B T}$, the slope of a linear regression line provides us directly with the activation energy E_a. We used the range from 8K to 28K as this is the domain where the values show linearity. Furthermore, we discarded two points that were obviously erroneous. Fig. 13 shows the entire plot with the regression line, the points we used for the line are marked in green color.

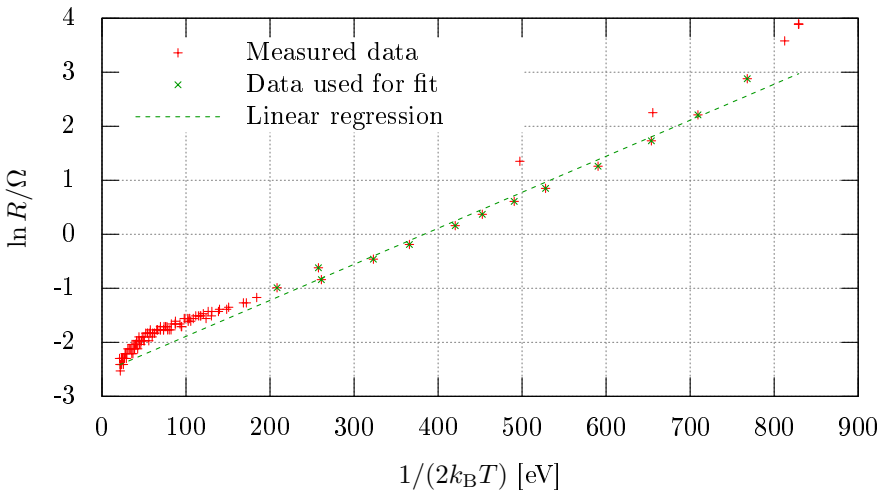

Figure 13: Activation energy of silicon

The slope is calculated as $S = (0.00667 \pm 0.00024)$eV so we found $E_a = 6.67$meV. As we do not know to which degree the silicon sample is doped with phosphorus, we can not compare this value with values in literature or in the manual.

5 Summary

We measured the resistances of a copper, a niobium and a phosphorous-doped silicon sample between 7K and 278K. We observed the expected temperature dependences: linear at high temperatures, then a curved shape and finally a constant residual resistance for metallic the copper and niobium sample with a transition to superconductivity (vanishing resistance for niobium at about 9K. For the silicon sample as semiconductor, the resistance was almost constant, indeed very slowly increasing with decreasing temperature and increased sharply at low temperatures.

We determined the residual resistances of copper ($R_{\mathrm{res,Cu}} = 0.02\Omega$) and niobium ($R_{\mathrm{res,Nb}} = 21.23\Omega$) and used these with the Grüneisen-Borelius-equation to calculate the Debye temperatures

and resistances. These are $\Theta_{\mathrm{Cu}} = 340.12\mathrm{K}$, $R_{\Theta,\mathrm{Cu}} = 2.65\Omega$, $\Theta_{\mathrm{Nb}} = 207.67\mathrm{K}$ and $R_{\Theta,\mathrm{Nb}} = 20.57\Omega$. We could verify the Grüneisen-Borelius-equation and found the powers of $R \propto T^p$ in the to be $p_{\mathrm{Cu}} = 4.65$ and $p_{\mathrm{Cu}} = 3.97$.

To obtain the mean free paths of the copper and niobium samples, we first calculated the specific resistances of copper $\rho_{\mathrm{Cu}}(4.2\mathrm{K}) = 1.48 \cdot 10^{-10}\Omega\mathrm{m}$ and niobium $\rho_{\mathrm{Nb}}(12\mathrm{K}) = 9.55 \cdot 10^{-8}\Omega\mathrm{m}$. The mean free paths are $\ell_{\mathrm{Cu},4.2\mathrm{K}} = 4.44\mu\mathrm{m}$ and $\ell_{\mathrm{Nb},12\mathrm{K}} = 3.93\mathrm{nm}$.

Further, we applied a magnetic field to the niobium sample to calculate the Ginsburg-Landau coherence length. We got $\xi_{\mathrm{GL}}^{(0)} = 9.15\mathrm{nm}$. Using this value, we could calculate the mean free path of niobium again, resulting in $\ell == 2.15\mathrm{nm}$. This is in the same range of magnitude but only almost half of the value obtained in the first place.

Finally, we calculated the activation energy of silicon by using the exponential dependence of the conductance on this energy: $E_{\mathrm{a}} = 6.67\mathrm{meV}$.

Appendix

- Graph of resistance on temperature for different magnetic fields and copy (2 sheets)
- Measurement data